Supporting Information – Bioconcentration assessment of three cationic surfactants in permanent fish cell lines

Fabian Balk[1,2], Bastian Hüsser[1,3], Juliane Hollender[1,3,§], Kristin Schirmer[1,2,3§*]

[1]Eawag, Swiss Federal Institute of Aquatic Science and Technology, 8600 Dübendorf, Switzerland
[2] EPF Lausanne, School of Architecture, Civil and Environmental Engineering, 1015 Lausanne, Switzerland
[3] ETH Zürich, Department of Environmental Systems Science, 8092 Zürich, Switzerland

*Corresponding author: Kristin.Schirmer@eawag.ch

[$] Both senior authors contributed equally to this work

31 pages, 10 figures and 25 tables

Contents

1. Test compound information

Table S1: Detail on the test compounds and their respective internal standards (CDN isotopes).

Compound	Acronym	CAS	MW g mol^{-1}	Density (g mL^{-1}, 20°C)	Vendor	Purity (%)
N-methyldodecylamine	S12	7311-30-0	199.38	0.791	Sigma-Aldrich	98
N,N-dimethyldecylamine	T10	1120-24-7	185.35	0.792	Sigma-Aldrich	97
N,N,N-trimethyltetradecylammonium ion	Q14	4574-04-3	256.49*	solid	Sigma-Aldrich	≥98
decyl-D_{21}-trimethylammonium ion	-	1515861-67-2	221.1*	solid	CDN Isotopes	99
Tetradecyl-D_{29}-trimethylammonium ion	-	95523-73-2	285.67*	solid	CDN Isotopes	99

* w/o salt

2. Conduction of bioconcentration experiments

In a first step, a test compound was directly dissolved in the exposure medium because all compounds were well soluble in aqueous solution without the aid of an organic solvent. The exposure medium consisted of L-15/FBS to sustain the metabolism of the cells [1, 2]. In a second step, the test compound stock solution was diluted to the final exposure concentration with additional L-15/FBS medium. This two-step dilution procedure was necessary to minimize variabilities in pipetting of small volumes or weighing small amounts of pure chemical (S12 and T10 liquid, Q14 solid at room temperature). To start an experiment, the routine cell culture medium was removed and replaced with 3 mL of the previously prepared L-15/FBS exposure medium.

The experimental design and sampling scheme of the bioaccumulation experiments was the same as detailed in Balk et al.[3] with minor adaptions. Exposed cells and cell-free negative control flasks were sampled at 0 h, 4 h, 8 h, 24 h, 48 h and 72 h, whilst a cell count control and a test compound-free control were sampled at experimental onset and termination. At each sampling time point, the medium, the cell surface, the cells themselves and test compound sorbed to plastic were sampled. Briefly, 1 mL exposure medium was sampled and the remaining 2 mL used for pH measurement (only every 24 h) using a small pH probe (microFET, Wellinq) or indicator strips (Macherey-Nagel). Then, 3 mL chemical- free L-15/FBS were added and the flask gently swayed for 30 seconds to reduce the carry-over from the exposure medium to the subsequent sample fractions. A 1 mL volume of the wash medium was sampled and combined with the first sample of exposure medium. Afterwards, the cell surface was rinsed with 400 µL Versene solution for 30 seconds. Versene contains the cell dissociation agent ethylenediaminetetraacetic acid (EDTA), which chelates with divalent metal ions [4]. Due to its four carboxylic acid groups with strong dissociation constants (pKa 0.26 to 2.76 [5]), EDTA is fully dissociated at pH 7 and able to associate with positively charged test compounds. Thus, any test compound loosely associated with the cell surface would have been sampled with the EDTA upon the rinse with Versene. Afterwards, the cell layer was sampled by the addition of 400 µL trypsin and scraping the cells with a cell scraper (Techno Plastic Products AG). An additional 400 µL trypsin added to the flask ensured the capture of the remaining cells and minimized carry over to the subsequent sample fraction. Both trypsin samples were combined and added to methanol containing internal standard. At last, the test compound sorbed to plastic was sampled by the addition of methanol-containing internal standard and shaken for 5 min at 200 rpm on a plate shaker. Each sample fraction was collected in a 15 mL centrifuge tube (91015, TPP Techno Plastic Products AG), which contained methanol with internal standard or, in case of the plastic sampling extract, ultrapure water (Honeywell Riedel-de

Haën). The sampling volumes were adapted such that the methanol fraction was 80% (v/v) in the sample, which ensured that test compound loss due to sorption to plastic or glass was minimized (SI section 5.1).

3. Mass balance derivation and *in vitro* BCF calculation

The mass balances were derived as described previously [3]. In brief, the $\%\ of\ total\ amount$ of each sample type (medium, cell surface, cells or plastic) was calculated as the quotient of the sample,Y_t, at the time point t over the sum of all sample types, $\sum Y_t$ (ng), at time point t, as shown in equation 1:

Equation S1 $$\%\ of\ total\ amount = \frac{Y_t}{\sum Y_t}\ .$$

The total amounts measured at each time point were compared to the initial total mass at 0 h to detect biotransformation activity or other losses. The calculation of *in vitro* BCFs was identical to our previous work, except for the differences in cell volume, cell number and cell weight for RTL-W1 and RTgill-W1 (SI also Table S6). Equation 2 describes the initial derivation of the cellular concentration of test compound, C_{cell}:

Equation S2: $$C_{cell}\ [\frac{ng}{L}] = \frac{cell\ _t\ [ng]}{mean\ cell\ number\ of\ experiment \times \left(\frac{1}{6} \times \pi \times d^{\,3}\right)\ [L]}\ ,$$

where the absolute amount of test compound, $cell\ _t$, at time point t, is divided by the volume of the cell layer, which depends on the measured cell number in the bioconcentration experiments and the cell diameter d. (see SI section 5.2 for metrics per chemical and cell line). We attempted to determine the time when steady state was reached in the experiments using a simple D_{OW}-based model , which, however, gave no realistic estimations. Since the model appeared to be inapplicable to cationic surfactants, we based our steady state estimations on the derived mass balances. Equation 3 was used to calculate the $in\ vitro\ BCF$, where C_{medium} was the averaged exposure concentration at apparent steady state of the test system (incl. all times points ≥24 h):

Equation S3: $$in\ vitro\ BCF = \frac{C_{cell}}{C_{medium}}$$

For comparison, we calculated D_{MLW} based predictions of BCFs in cells, termed $D_{MLW}BCF$, which used the cells' volume fractions of phospholipid, $v_{Phospholipid}$, the compound's D_{MLW}, averaged cell weight, w [g] (Table S6), the weight-based phospholipid fraction, f_{PL} (0.01)[6], its density, ρ_{PL} [g L^{-1}] (1.0138 kg L^{-1})[7], and the cell volume multiplied by the measured cell number, V_{cell} [L] (Table S6):

Equation S4: $$D_{MLW}BCF = 10^{logD_{MLW}} \times v_{Phospholipid} = 10^{logD_{MLW}} \times \frac{\frac{w \times f_{PL}}{\rho_{PL}}}{V_{cell}}$$

A detailed desription of the derivation is available in the SI of our earlier work [3].

4. Chemical analysis

4.1. Mass spectrometer settings

For sample quantification, an LCMS/MS system was applied. Positive full scan MS at a resolution of 140 000 at m/z 200 (120 000 for Exploris) with data-dependent MS2 acquisition,

with a resolution of 17 500 (30 000 for Exploris) and an isolation window of 1 m/z, were recorded for all test compounds. Standard calibrations in ultrapure water containing 80% methanol and internal standards were used for quantification. Each sample run was 20 minutes long. The eluent ramp with a flow of 200 µL min^{-1} began with 10% of methanol, which was increased to 95% after 3 minutes and kept at 95% from 14 to 17 minutes. Afterwards, the methanol fraction was decreased within a minute and brought down to 10 % from 18 minutes onward until the end of the measurement. The column temperature was set to 40°C. Ionization of the target analytes was achieved by electrospray ionization (ESI) with a spray voltage of + 4kV in positive mode while the ion transfer capillary was heated to 320 °C. Full scan acquisitions were performed at a range of 50 to 630 m/z and top 5 data-dependent MS/MS conducted based on an inclusion list containing all test compounds along with their suspected and known biotransformation products. Data acquisitions were analyzed with the Software Tracefinder 4.1 (Thermo Fisher Scientific). Collision energies and m/z are listed in Table S2, while in Table S4 and Table S5 the limit of quantification (LOQ) and the matrix specific relative recoveries are presented, respectively.

Table S2: Test compound's m/z and collision energies. Please note that we measured samples with three different mass spectrometers, QExactive and Exploris. All targets were measured in positive mode.

Compound	Mass (m/z)	Fragment Ions m/z	Normalized collision energy (QExactives)	Normalized collision energy (Exploris)
N-methyldodecylamine (S12)	200.2373	57.030, 71.0862, 85.050	60	65
N,N-dimethyldecylamine (T10)	186.2216	57.0707, 71.010, 85.050	70	75
N,N,N-trimethyltetradecylammonium (Q14)	256.2999	57.090, 60.081, 71.000	60	65

4.2. Screening for biotransformation products

The mass balances of bioconcentration experiments were used to test if criteria for biotransformation activity according to OECD TG319 [8,9] were met. Also, we conducted a screening for potential and known biotransformation products in the media and cell samples. A suspect list was created based on biotransformation products known from literature [10,11]. Detected candidates had to be present in either media or cell samples and be absent in any of the control samples (compound-free or cell-free controls). Further, the candidates had to show temporal trends in peak intensities over the experimental duration and peak intensities had to be ≥ 0.1 % compared to their parent compound. The settings for detection of biotransformation products are presented in Table S3.

Table S3: Compound Discoverer settings for peak detection of suspected biotransformation products.

Setting	
Minimal Peak intensity	1.00E+06
Minimal fold difference Sample/Control	5
Possible Phase I reactions for suspect BTP generation	Dealkylation; Desaturation (H2 ->); Oxidation (-> O); Oxidative Deamination to Alcohol (H2 N -> H O); Oxidative Deamination to Ketone (H3 N -> O); Reduction (-> H2)
Possible Phase II reactions for suspect BTP generation	Dealkylation; Acetylation (H -> C2 H3 O); Arginine Conjugation (H O -> C6 H13 N4 O2); Cysteine Conjugation 1 (H -> C3 H6 N O2 S); Cysteine Conjugation 2 (-> C3 H7 N O2 S); Glucoside Conjugation (H -> C6 H11 O5); Glucuronide Conjugation (H -> C6 H9 O6); Glutamine Conjugation (H O -> C5 H9 N2 O3); Glycine Conjugation (H O -> C2 H4 N O2); GSH Conjugation 1 (-> C10 H15 N3 O6 S); GSH Conjugation 2 (-> C10 H17 N3 O6 S); Methylation (H -> C H3); Ornitine Conjugation (H O -> C5 H11 N2 O2); Palmitoyl Conjugation (H -> C16 H31 O); Stearyl Conjugation (H -> C18 H35 O); Sulfation (H -> H O3 S); Taurine Conjugation (H O -> C2 H6 N O3 S)
m/z tolerance	5 ppm
Average Peak width	automated detection

4.3. Performance of chemical analysis

Table S4: Limit of quantification of test compounds and comparison of intended vs. measured exposure concentration in bioconcentration experiments. * lowest LOQ given, depending on measurement sequence it ranged from 50 to 1000 ng L^{-1}, **geometric mean of stock solutions sampled at experimental onset and termination.*** The doubled exposure concentration vs. nominal for T10 was thought to be caused by pipetting errors in the preparation of stock solutions, which was diluted two times to obtain the final exposure concentration.

Compound	Cell line	LOQ (µg L^{-1})*	Nominal exposure C (µg L^{-1})	% of nominal exposure C ± SD**
N-methyldodecylamine (S12)	RTgill-W1	0.050	200	112 ± 11
N-methyldodecylamine (S12)	RTL-W1	0.050	200	92 ± 13
N,N-dimethyldecylamine (T10)	RTgill-W1	0.050	185	195 ± 86***
N,N-dimethyldecylamine (T10)	RTL-W1	0.050	185	210 ± 40***
N,N,N-trimethyltetradecylammonium (Q14 R1)	RTgill-W1	0.050	100	86 ± 1
N,N,N-trimethyltetradecylammonium (Q14 R2)	RTL-W1	0.050	20	112 ± 11

Table S5: Matrix specific relative recoveries of the test compounds.

Compound	relative recovery - Medium (%)	relative recovery - Surface (%)	relative recovery - Cell (%)	relative recovery - Plastic (%)
N-methyldodecylamine (S12)	106	102	119	110
N,N-dimethyldecylamine (T10)	96	104	100	96
N,N,N-trimethyltetradecylammonium (Q14)	114	185	100	100

5. Experimental optimizations

5.1. Compound adsorption in experimental set up

This experiment was conducted with a range of methanol percentages (v/v) to monitor the absorption of the test compounds to the walls of either glass or plastic vials (Figure S1). The mixtures were sampled after 24 hours, at which the system was assumed to have reached chemical equilibrium. Clear differences between absorption affinity to glass or plastic were seen for S12 for methanol percentages < 80 % (left pane Figure S1). Therefore, we decided to use a methanol percentage of 80 % in the sampling for bioconcentration assessments.

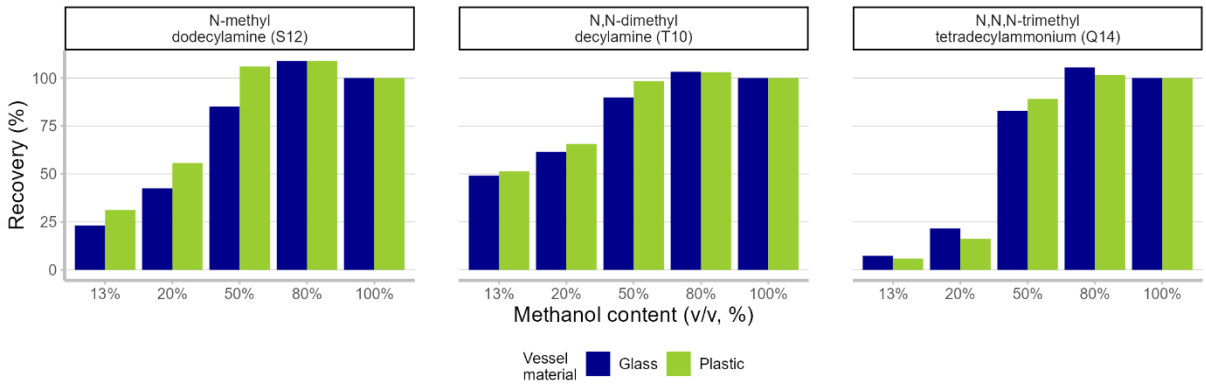

Figure S1: Absorption experiment of test compounds to glass or plastic vials in varying water-methanol mixtures.

5.2. Optimal seeding density for bioconcentration assessment

We tested two different cell densities of RTgill-W1 in cell culture flasks (25 cm^2 growth area), to ensure minimal variability in cell numbers over the experimental duration of bioconcentration experiments (Figure S3). We assumed a negligible difference between the 48 h and 72 h experimental duration. The cell density of $4.6x10^6$ cells/flask was chosen as the seeding density for all bioconcentration experiments with RTgill-W1, since the variability was smaller than in the higher cell density of $5.6x10^6$ cells/flask.

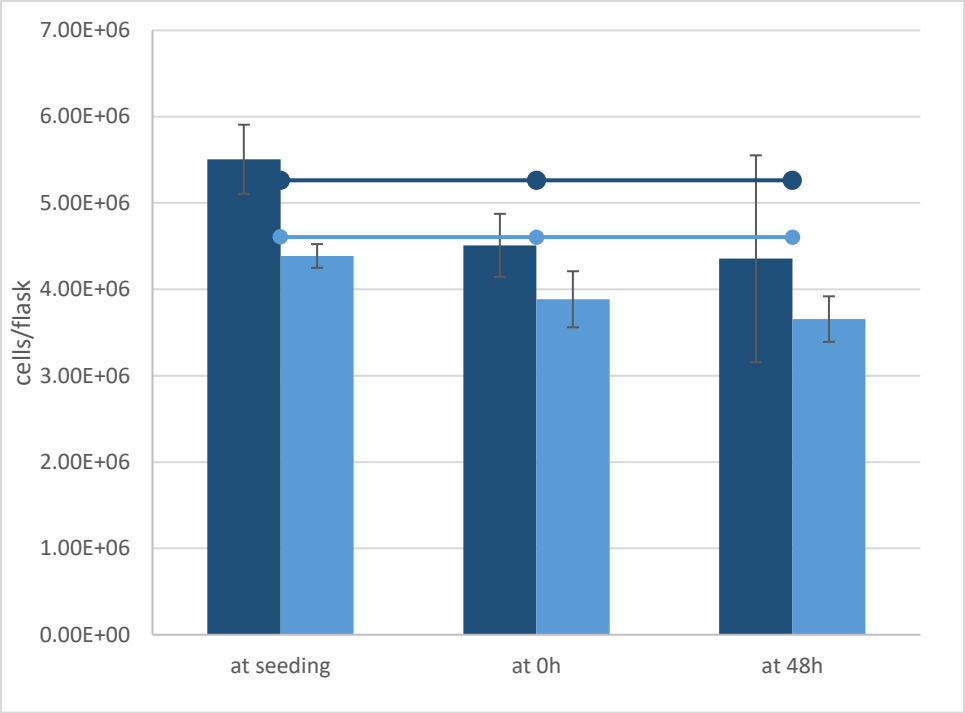

Figure S2: Cell numbers of RTgill-W1 in two tested densities over 48 h relative to the intended cell number. We assumed a negligible difference of the cell numbers between 48 h and 72 h experimental duration. Each density was measured in three biological replicates. Error bars are standard deviations, while the horizontal lines mark the intended seeding density. Dark blue columns = Actual seeded cells with $5.3x10^6$ cell/flask, Light blue column = Actual seeded cells with $4.6x10^6$ cells/flask, dark/light blue line = intended theoretical cell number over the test duration ($5.3x10^6$ cell/flask and $4.6x10^6$, respectively)

In each experiment, the exposed cells were counted at experimental onset and termination. The cell numbers are documented in Table S6. They were used for calculation of cell internal concentrations of the test compounds according to the method by Stadnicka-Michalak et al.[1] and Balk et al.[3].

Table S6: Cell numbers per test compound and cell line. Besides the cell numbers, the following metrics were needed for accumulation predictions. RTL-W1 cell diameter: 16.6 µm, volume: $2.4×10^{-12}$ L $cell^{-1}$, weight: $2.4×10^{-9}$ g $cell^{-1}$; RTgill-W1 cell diameter: 15.1 µm, volume: $1.8×10^{-12}$ L $cell^{-1}$, weight: $1.8×10^{-9}$ g $cell^{-1}$, be = bioconcentration experiment, be+rp = bioconcentration experiment+re-equilibration phase

Compound	Experiment	Cell	Mean cell number (0 h and 72 h)	Standard deviation	Total cell weight (g, mean)
S12	be	RTgill-W1	6400200	1742245	0.0115
S12	be	RTL-W1	3715200	279050	0.007
T10	be	RTgill-W1	6471867	1787199	0.012
T10	be	RTL-W1	3766720	688284	0.007
Q14	be+rp	RTL-W1	3041675	666557	0.005
Q14	be	RTgill-W1	7050000	400327	0.013

T10	be+rp	RTL-W1	3023600	1049162	0.005

6. Cytotoxicity data

6.1. Concentration-response curves

The concentration-response curves presented in Figure S3 and the concurrent measured exposure concentrations in Table S7 were used to derive EC_{50} values and non-toxic exposure concentrations for later bioconcentration experiments.

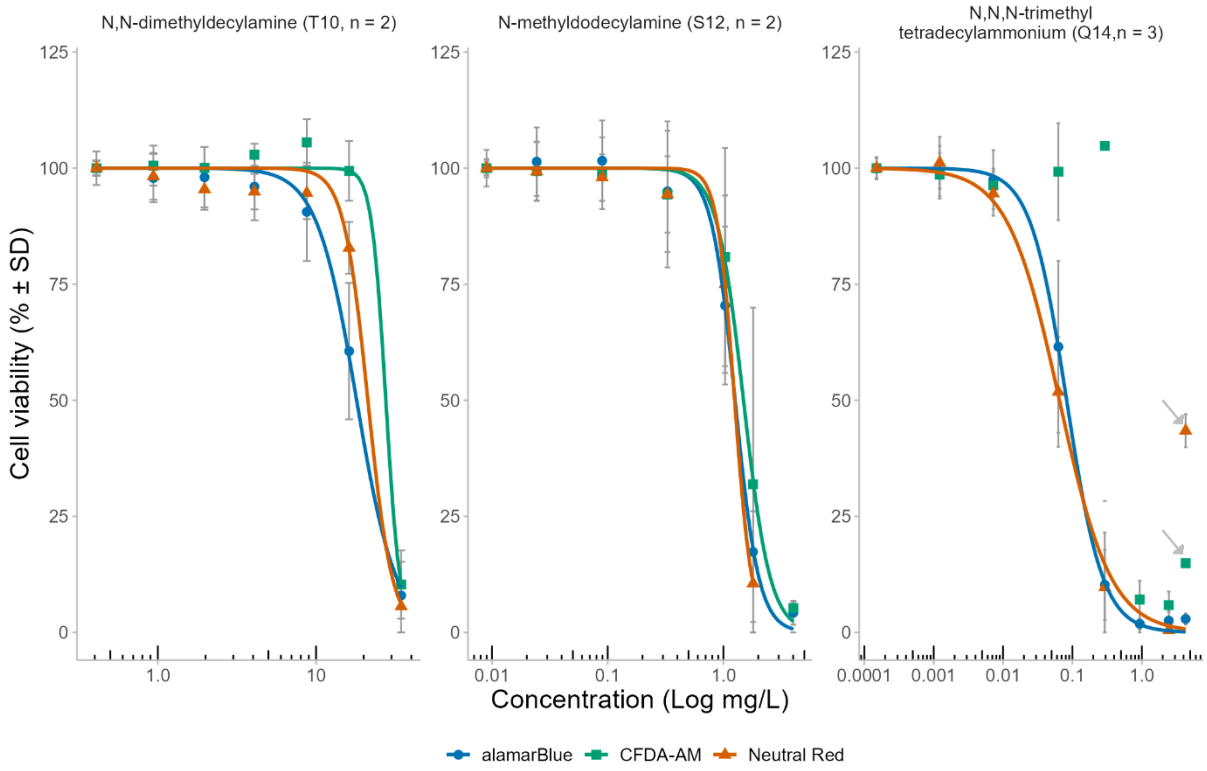

Figure S3: Percent cell viability relative to unexposed control as measured by alamarBlue™, CFDA-AM and Neutral Red upon 24 h exposure of the test compounds to RTgill-W1. The highest concentration of *N,N,N*-trimethyltetradecylammonium caused a fluorescence interference with Neutral Red and CFDA-AM (indicated by arrows) and the concentration-response curve of the CFDA-AM could not be fitted. The comparisons of nominal and measured exposure concentrations are presented in Table S7. Error bars are the standard deviation across all biological replicates. n = number of biological replicates, CFDA-AM = 5-carboxyfluorescein diacetate acetoxy methyl ester

Table S7: Nominal and measured exposure concentrations of the acute cytotoxicity assays. The measured geometric mean based on all biological replicates and their medium samples taken at 0h and 24h of exposure.

Test compound	Nominal concentration (mg L^{-1})	Measured concentration (±SD, 0 h)	Measured concentration (±SD, 24 h)	Measured geometric mean (mg L^{-1})	Measured vs. nominal concentration (%)
S12	0.125	0.03 ± 0.00	0.003 ± 0.000	0.009 ± 0.01	7
S12	0.25	0.07 ± 0.00	0.008 ± 0.000	0.02 ± 0.04	10
S12	0.5	0.2 ± 0.1	0.04 ± 0.02	0.09 ± 0.09	18
S12	1	0.56 ± 0.10	0.2 ± 0.0	0.33 ± 0.20	33
S12	2	1.4 ± 0.4	0.8 ± 0.1	1 ± 0.4	52
S12	3	2.2 ± 0.4	1.5 ± 0.3	1.8 ± 0.5	60
S12	6	4.6 ± 0.7	3.6 ± 0.6	4 ± 0.8	67
T10	1.125	0.5 ± 0.1	0.32 ± 0.04	0.4 ± 0.1	36
T10	2.25	1.2 ± 0.2	0.8 ± 0.1	0.9 ± 0.3	42
T10	4.5	2.3 ± 0.4	1.7 ± 0.1	2 ± 0.4	44
T10	9	4.8 ± 1	3.5 ± 0.3	4.1 ± 0.1	45
T10	18	10.7 ± 0.6	7.2 ± 0.6	8.7 ± 2.1	49
T10	36	19 ± 2.2	13.8 ± 0.5	16.2 ± 3.3	45
T10	74	41 ± 5.3	29 ± 0.5	34.5 ± 7.8	47
Q14	0.06	0.0002 ± 0.000	0.0002 ± 0.000	0.0002 ± 0.000	0
Q14	0.11	0.005 ± 0.004	0.0009 ± 0.0010	0.001 ± 0.004	1
Q14	0.22	0.02 ± 0.01	0.003 ± 0.001	0.007 ± 0.01	3
Q14	0.44	0.13 ± 0.07	0.03 ± 0.01	0.1 ± 0.1	14
Q14	0.88	0.6 ± 0.4	0.17 ± 0.02	0.3 ± 0.3	33
Q14	1.75	1.6 ± 1.0	0.6 ± 0.2	0.9 ± 0.8	53
Q14	3.5	3.7 ± 2.1	1.8 ± 0.4	2.5 ± 1.7	70
Q14	7	4.9*	3.7*	4.3 ± 0.8	61
*only one replicate tested at this concentration					

Table S8: Percent cell viability and corresponding nominal exposure concentrations of the acute cytotoxicity assays after 24 h exposure. AB = alamarBlue™ (metabolic activity), CFDA-AM = 5-carboxyfluorescein diacetate acetoxy methyl ester (cell membrane integrity), NR = Neutral Red (lysosomal membrane integrity), SD = Standard Deviation

Test compound	Nominal concentration (mg L^{-1})	AB (± SD, %)	CFDA-AM (± SD, %)	Neutral Red (± SD, %)
S12	0	100	100	100
S12	0.125	100 ± 2	100 ± 4	100 ± 1
S12	0.25	101 ± 7	99 ± 6	99 ± 6
S12	0.5	102 ± 9	99 ± 8	98 ± 5
S12	1	95 ± 13	94 ± 8	94 ± 16
S12	2	70 ± 17	81 ± 24	75 ± 19
S12	3	17 ± 15	32 ± 38	11 ± 16
S12	6	4 ± 3	5 ± 1	0 ± 2
T10	0	100	100	100
T10	1.125	100 ± 4	100 ± 2	100 ± 1
T10	2.25	98 ± 5	101 ± 4	98 ± 5
T10	4.5	98 ± 7	100 ± 4	95 ± 4
T10	9	98 ± 7	103 ± 2	95 ± 4
T10	18	91 ± 11	106 ± 5	95 ±6
T10	36	61 ± 15	99 ± 6	83 ± 6
T10	74	8 ± 3	10 ± 7	6 ± 10
Q14	0	100	100	100
Q14	0.06	100 ± 2	100 ± 2	100 ± 2
Q14	0.11	99 ± 6	99 ± 5	101 ± 6
Q14	0.22	98 ± 6	96 ± 4	95 ± 5
Q14	0.44	62 ± 19	99 ± 10	52 ± 12
Q14	0.88	10 ± 8	105 ± 77	10 ± 12
Q14	1.75	2 ± 1	7 ± 4	0 ± 3
Q14	3.5	3 ± 2	6 ± 3	0 ± 2
Q14	7	2.9 ± 1	15 ± 0.3	43 ± 3

6.2. Cell viability on test compound exposure for bioconcentration experiments

Figure S4 shows the viability (%) after exposure to the test compound concentrations intended for the bioconcentration experiments relative to the test compound-free control. Q14 was initially tested at 100 µg L^{-1} in the absence of fetal bovine serum (FBS) in the L15/ex medium as a worst case-scenario, which resulted in approximately 30 to 40% toxicity in RTgill-W1 after 72 h of exposure. When instead 20 µg L^{-1} of Q14 and L15/ex medium with FBS was used, percent viability in the exposed cells remained comparable to the control.

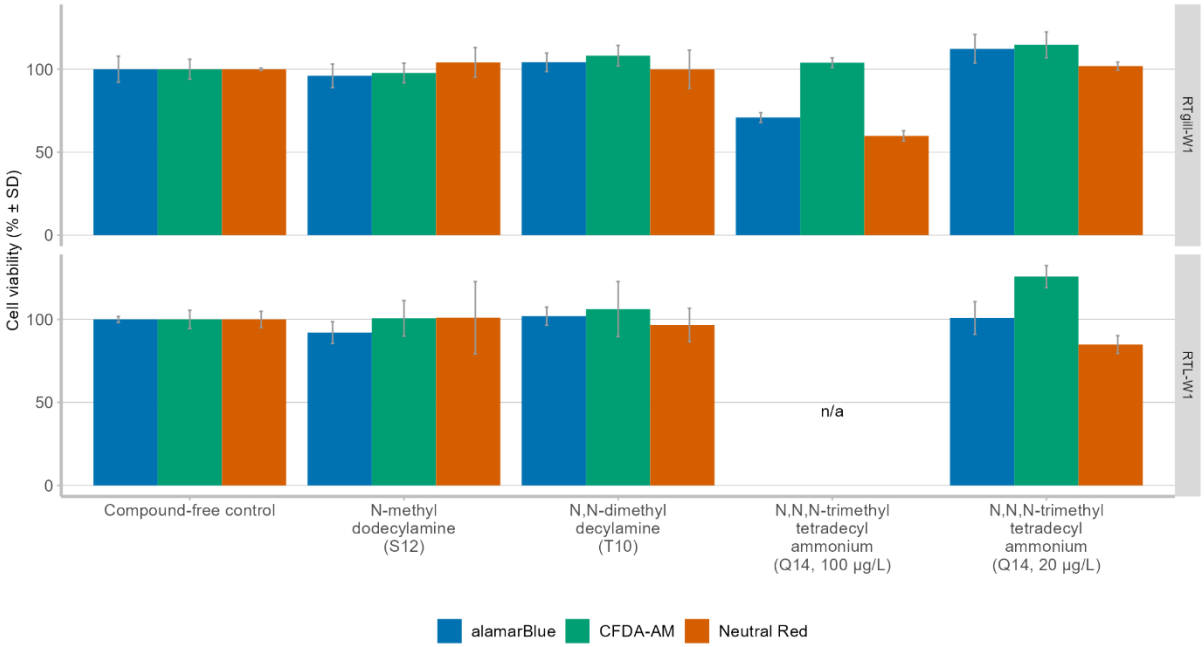

Figure S4: Impact on cell viability of the exposure concentrations used in bioconcentration assessments after 72 h. alamarBlue indicates metabolic activity, CFDA-AM cell membrane integrity and Neutral Red lysosomal membrane integrity. Error bars indicate the standard deviation of the two biological replicates. Please note that the first and second replicate of *N,N,N*-trimethyltetradecylammonium are presented separately due to the use of different exposure concentrations in experiments with RTgill-W1 (error bars represent technical replicates in this case). n/a = not applicable, since 20 µg L^{-1} exposures of Q14 were not used in RTL-W1 cell cultures.

Table S9 shows the compound concentrations measured in the cytotoxicity assay (Figure S4). It was observed that the exposure concentration was consistently lower than the nominal concentration. The test compounds likely were taken up by the cells as well as adsorbed to the plastic in the cytotoxicity assay, which lowered the measured medium concentrations relative to the nominal exposure concentration. This effect can be seen most clearly for the second replicate of Q14 (Q14R2, Table S9).

Table S9: Measured concentrations (C_{0h} and C_{72h}) of the cytotoxicity assay with final exposure concentrations for bioconcentration experiments. Shown are the measured medium concentrations (geometric mean of experimental start, C_{0h}, and termination, C_{72h}) of the two biological replicates of each cell line and the cell-free control. S12 = *N*-methyldodecylamine, T10 = *N,N*-dimethyldecylamine, Q14 = *N,N,N*-trimethyltetradecylammonium, R1 = replicate 1, R2 = replicate 2, SD = Standard deviation

Compound	Cell line	Nominal concentration (µg L^{-1})	Concentration (± SD, 0h)	Concentration (± SD, 72h)	Geometric mean (measured, µg L^{-1})	SD (measured, µg L^{-1})	Percent of nominal
S12	cell-free	200	274 ± 50	243 ± 34	257	44	129
S12	RTgill-W1	200	237 ± 20	42 ± 12	100	103	50
S12	RTL-W1	200	255 ± 24	86 ± 14	148	90	74
T10	cell-free	185	171 ± 30	158 ± 38	164	34	89
T10	RTgill-W1	185	166 ± 34	133 ± 29	149	35	80
T10	RTL-W1	185	168 ± 31	141 ± 38	154	36	83
Q14R1	cell-free	100	144 ± 29	117 ± 32	130	31	130
Q14R1	RTgill-W1	100	141 ± 4	22 ± 1	56	65	56
Q14R1	RTL-W1	100	136 ± 14	35 ± 3	69	56	69
Q14R2	cell-free	20	4 ± 3	2 ± 4	3	3	14
Q14R2	RTgill-W1	20	5 ± 0.4	0.8 ± 0.02	2	2	12
Q14R2	RTL-W1	20	5 ± 0.6	0.9 ± 0.05	2	2	11

7. Bioconcentration experiments

7.1. pH measurements

Most of the samples were measured with pH indicator strips, which allowed for rough pH measurement in steps of 0.5 pH units (Figure S5).

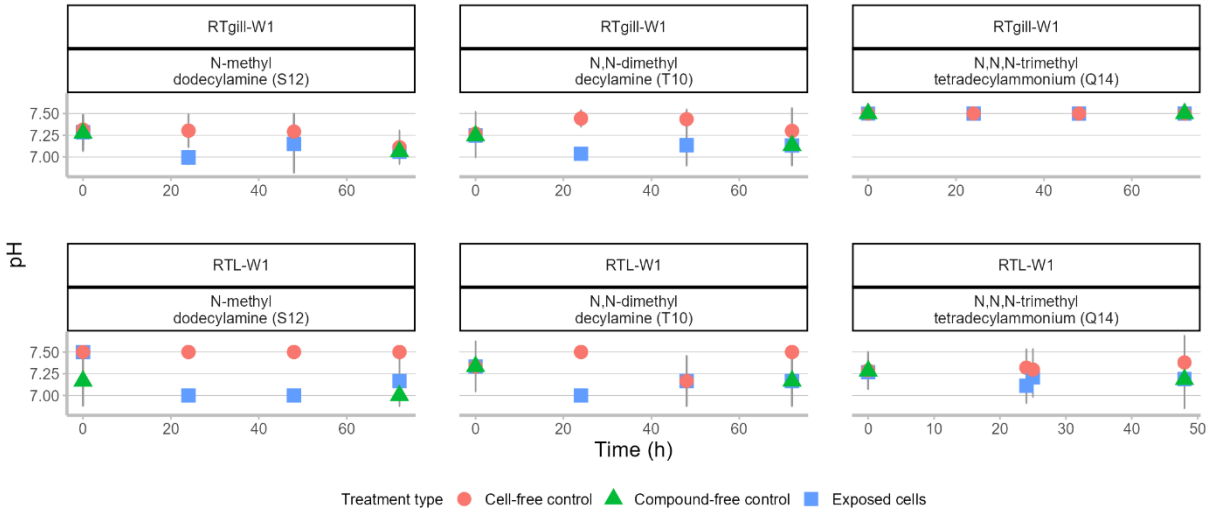

Figure S5: pH measurements of exposed cells and controls over the experimental duration. The pH was measured every 24 h. Error bars indicate the standard deviation across the biological replicates.

7.2. Mass balances

Tables S10 to S13 show the mass balances of the bioconcentration experiments. Where no standard deviations are documented, the experiment was conducted only once. Experiments are distinguished as bioconcentration experiments and bioconcentration experiments that contain a re-equilibration phase with test compound-free medium (see table captions below). It is possible that the cell surface sampling in the cell-free controls sampled test compound adsorbed to plastic. This explained the partially higher test compound amounts of cell surface samples in the cell-free controls relative to the exposed cells.

Table S10: Mass balances of RTgill-W1 and RTL-W1 cells and cell-free controls exposed to S12 in bioconcentration experiments. At the 72 h time point, samples were spiked to calculate relative recoveries. Consequently, the sample amount was split into a spiked sample and a sample for comparison. This resulted in different dilutions relative to samples from other time points, which we accounted for in our calculation of the concentrations and absolute amounts. However, any differences that occurred for the 72 h samples relative to the other time points are likely an artefact from the different sample dilutions. The spikes were not high enough and no relative recovery could be calculated. Therefore, a separate spike experiment was conducted, see Table S5.

Cell line	Sample Type	Time point (h)	Absolute amount (exposed cells, ng)	Standard deviation (exposed cells, ng)	Absolute amount (cell-free control, ng)	Standard deviation (cell-free control, ng)
RTgill-W1	CELL	0	204	23	5	2
RTgill-W1	CELL	4	418	69	12	10
RTgill-W1	CELL	8	442	25	3	3
RTgill-W1	CELL	24	375	39	5	1
RTgill-W1	CELL	48	412	34	4	1
RTgill-W1	CELL	72	465	200	5	1
RTgill-W1	MEDIUM	0	433	164	440	14
RTgill-W1	MEDIUM	4	165	175	434	97
RTgill-W1	MEDIUM	8	55	24	443	95
RTgill-W1	MEDIUM	24	39	12	400	24
RTgill-W1	MEDIUM	48	34	11	391	41
RTgill-W1	MEDIUM	72	25	7	372	19
RTgill-W1	PLASTIC	0	32	28	130	46
RTgill-W1	PLASTIC	4	74	55	151	52
RTgill-W1	PLASTIC	8	59	49	154	58
RTgill-W1	PLASTIC	24	90	78	161	59
RTgill-W1	PLASTIC	48	67	40	165	49
RTgill-W1	PLASTIC	72	28	27	172	75
RTgill-W1	SURFACE	0	2	0.20	7	2
RTgill-W1	SURFACE	4	2	0.30	5	1
RTgill-W1	SURFACE	8	2	0.30	5	0.1
RTgill-W1	SURFACE	24	2	0.30	5	1
RTgill-W1	SURFACE	48	1	0.60	5	1
RTgill-W1	SURFACE	72	1	0.80	5	2
RTL-W1	CELL	0	162	20	4	4
RTL-W1	CELL	4	354	47	4	3
RTL-W1	CELL	8	369	51	3	3
RTL-W1	CELL	24	365	31	3	2
RTL-W1	CELL	48	370	51	3	2
RTL-W1	CELL	72	292	50	3	3
RTL-W1	MEDIUM	0	346	54	416	80
RTL-W1	MEDIUM	4	87	10	389	62
RTL-W1	MEDIUM	8	78	7	400	57
RTL-W1	MEDIUM	24	60	8	371	66
RTL-W1	MEDIUM	48	47	1	363	74

RTL-W1	MEDIUM	72	37	4	349	59
RTL-W1	PLASTIC	0	14	13	106	25
RTL-W1	PLASTIC	4	28	25	108	39
RTL-W1	PLASTIC	8	28	24	116	44
RTL-W1	PLASTIC	24	23	20	118	22
RTL-W1	PLASTIC	48	27	23	123	28
RTL-W1	PLASTIC	72	13	11	123	33
RTL-W1	SURFACE	0	3	1	5	1
RTL-W1	SURFACE	4	6	1	5	1
RTL-W1	SURFACE	8	4	0.4	4	0.2
RTL-W1	SURFACE	24	2	0.3	3	0.3
RTL-W1	SURFACE	48	2	1	4	0.4
RTL-W1	SURFACE	72	1	1	4	1

Table S11: Mass balances of RTgill-W1 and RTL-W1 cells and cell-free controls exposed to T10 in bioconcentration experiments. At the 72 h time point, samples were spiked to calculate relative recoveries. Consequently, the sample amount was split into a spiked sample and a sample for comparison. This resulted in different dilutions relative to samples from other time points, which we accounted for in our calculation of the concentrations and absolute amounts. However, any differences that occurred for the 72 h samples relative to the other time points are likely an artefact from the different sample dilutions. The spikes were not high enough and no relative recovery could be calculated. Therefore, a separate spike experiment was conducted, see Table S5.

Cell line	Sample Type	Time point (h)	Absolute amount (exposed cells, ng)	Standard deviation (exposed cells, ng)	Absolute amount (cell-free control, ng)	Standard deviation (cell-free control, ng)
RTgill-W1	CELL	0	215	76	3	5
RTgill-W1	CELL	4	322	104	4	7
RTgill-W1	CELL	8	312	61	4	6
RTgill-W1	CELL	24	364	110	17	22
RTgill-W1	CELL	48	338	78	4	5
RTgill-W1	CELL	72	196	197	2	4
RTgill-W1	MEDIUM	0	800	512	1099	588
RTgill-W1	MEDIUM	4	724	470	1065	543
RTgill-W1	MEDIUM	8	713	450	1042	545
RTgill-W1	MEDIUM	24	622	472	945	572
RTgill-W1	MEDIUM	48	578	464	890	573
RTgill-W1	MEDIUM	72	433	321	855	551
RTgill-W1	PLASTIC	0	55	17	114	34
RTgill-W1	PLASTIC	4	110	17	169	31
RTgill-W1	PLASTIC	8	114	38	192	40
RTgill-W1	PLASTIC	24	125	18	207	7
RTgill-W1	PLASTIC	48	140	16	221	52
RTgill-W1	PLASTIC	72	62	22	211	24
RTgill-W1	SURFACE	0	22	18	6	11
RTgill-W1	SURFACE	4	30	26	8	15
RTgill-W1	SURFACE	8	28	27	7	11
RTgill-W1	SURFACE	24	18	21	17	30
RTgill-W1	SURFACE	48	14	22	6	11
RTgill-W1	SURFACE	72	37	61	7	12
RTL-W1	CELL	0	230	65	6	5
RTL-W1	CELL	4	289	77	7	6
RTL-W1	CELL	8	289	80	6	5
RTL-W1	CELL	24	344	105	5	5
RTL-W1	CELL	48	349	54	8	9
RTL-W1	CELL	72	286	63	0	0

RTL-W1	MEDIUM	0	898	118	1141	181
RTL-W1	MEDIUM	4	876	182	1124	211
RTL-W1	MEDIUM	8	875	166	1092	189
RTL-W1	MEDIUM	24	706	112	1032	187
RTL-W1	MEDIUM	48	635	152	921	198
RTL-W1	MEDIUM	72	475	137	808	200
RTL-W1	PLASTIC	0	28	13	91	31
RTL-W1	PLASTIC	4	77	12	156	19
RTL-W1	PLASTIC	8	100	29	165	48
RTL-W1	PLASTIC	24	88	27	181	40
RTL-W1	PLASTIC	48	138	21	203	24
RTL-W1	PLASTIC	72	46	1	239	14
RTL-W1	SURFACE	0	34	15	17	16
RTL-W1	SURFACE	4	40	18	18	15
RTL-W1	SURFACE	8	37	16	17	16
RTL-W1	SURFACE	24	30	15	16	17
RTL-W1	SURFACE	48	21	24	15	17
RTL-W1	SURFACE	72	47	29	17	17

Table S12: Mass balances of RTgill-W1 cells and cell-free controls exposed to Q14 in one bioconcentration experiment. At the 72 h time point, samples were spiked to calculate relative recoveries. Consequently, the sample amount was split into a spiked sample and a sample for comparison. This resulted in different dilutions relative to samples from other time points, which we accounted for in our calculation of the concentrations and absolute amounts. However, any differences that occurred for the 72 h samples relative to the other time points are likely an artefact from the different sample dilutions. The spikes were not high enough and no relative recovery could be calculated. Therefore, a separate spike experiment was conducted, see Table S5.

Sample Type	Time point (h)	Absolute amount (exposed cells, ng)	Absolute amount (cell-free control, ng)
CELL	0	20	0
CELL	4	208	0
CELL	8	258	0
CELL	24	259	0
CELL	48	266	0
CELL	72	202	0
MEDIUM	0	228	198
MEDIUM	4	45	168
MEDIUM	8	16	163
MEDIUM	24	9	167
MEDIUM	48	5	164
MEDIUM	72	4	145
PLASTIC	0	8	67
PLASTIC	4	23	87
PLASTIC	8	17	90
PLASTIC	24	14	94
PLASTIC	48	17	89
PLASTIC	72	19	85
SURFACE	0	1	1
SURFACE	4	0.2	1

SURFACE	8	0.2	1
SURFACE	24	0.1	1
SURFACE	48	0.1	1
SURFACE	72	0.2	1

Table S13: Mass balances of RTL-W1 cells and cell-free controls exposed to Q14 in bioconcentration experiments containing a re-equilibration phase. <LOQ = below limit of quantification**:** Samples were corrected for Q14-free controls, which were close to measured concentrations in the medium samples of the depuration phase. Therefore, it is possible that it appeared here like a decreasing medium concentration over time rather than variabilities in medium concentrations, which were lower than background concentrations of the Q 14-free controls.

Sample Type	Time point (h)	Absolute amount (exposed cells, ng)	Standard deviation (exposed cells, ng)	Absolute amount (cell-free control, ng)	Standard deviation (cell-free control, ng)
CELL	0	36	36	0	0
CELL	24	47	55	0	0
CELL	25	73	13	0	0
CELL	27	75	12	0	0
CELL	30	72	9	0	0
CELL	48	74	13	0	0
MEDIUM	0	56	2	45	10
MEDIUM	24	1.4	2	30	0
MEDIUM	25	1	1	9	0
MEDIUM	27	1	1	5	7
MEDIUM	30	<LOQ	-	11	6
MEDIUM	48	<LOQ	-	11	2
PLASTIC	0	3	0.4	28	1
PLASTIC	24	5	0.2	42	6
PLASTIC	25	4	1	33	5
PLASTIC	27	4	0	31	5
PLASTIC	30	4	1	29	5
PLASTIC	48	3	1	26	5
SURFACE	0	0	0	0	0
SURFACE	24	0	0	0	0
SURFACE	25	0	0	0	0
SURFACE	27	0	0	0	0
SURFACE	30	0	0	0	0
SURFACE	48	0	0	0	0

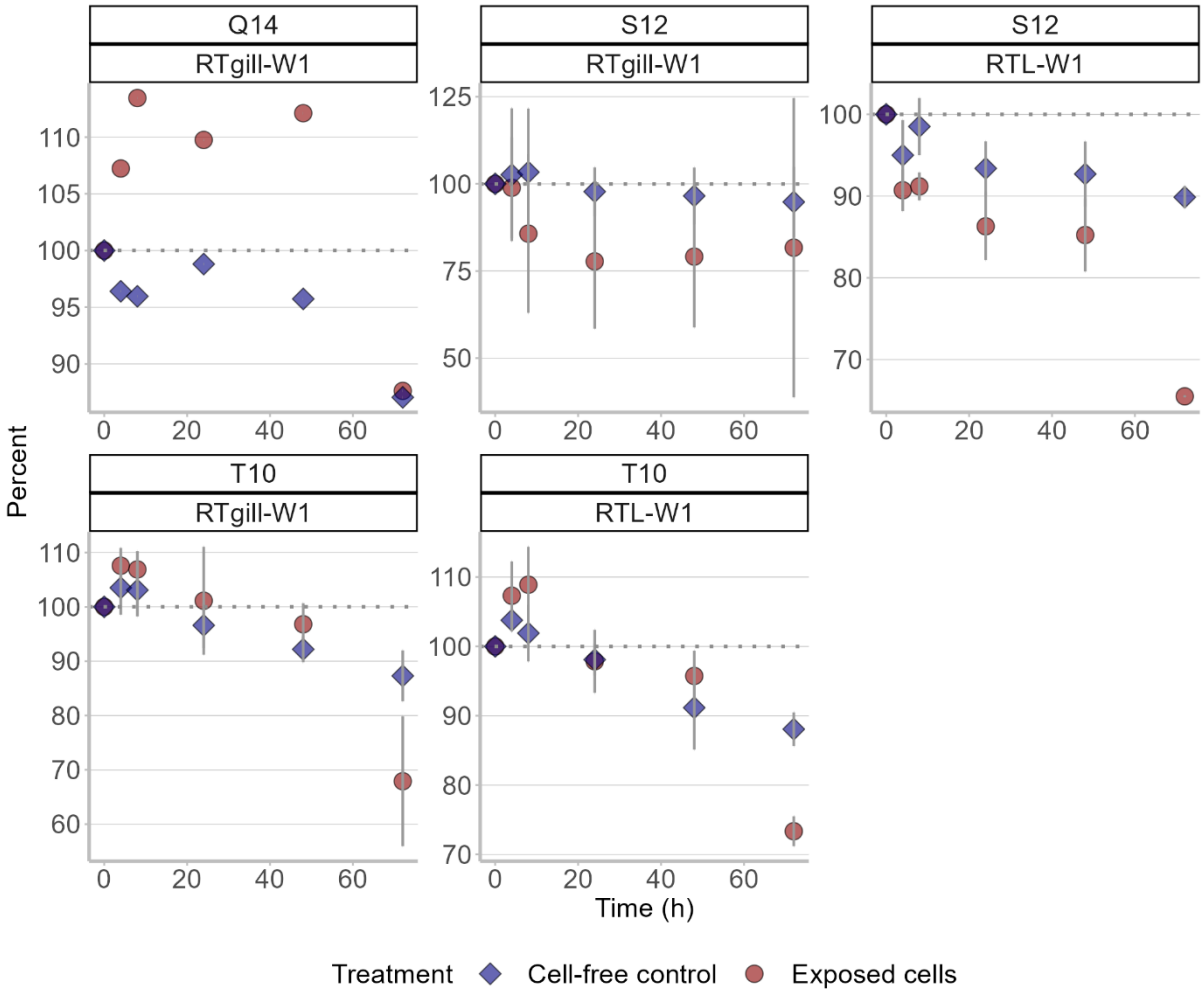

Figure S6: Mass balances of the bioconcentration experiments relative to the intial mass at 0 h. Please note, that the mass balance for the re-equilibration experiment with Q14 in RTL-W1 is not depicted, since the full mass balance was only available for 2 time points (0h and 24h, medium exchange after 24 h). The depicted experiment with Q14 was conducted once, therefore no standard deviations could be calculated. As noted in Table S10 –S12 above, the consistently lower masses at 72 h are thought to be an experimental artefact and not biotic or abiotic compound loss. The grey dotted line marks the theoretical 100 % mass balance, while the vertical lines mark the standard deviation. Please note, that some standard deviations may be covered by the symbols.

7.3. *In vivo*, *in vitro* and partition coefficient-based BCF

Table S14 shows the BCF calculation using different approaches to understand the observed *in vitro* and *in vivo* bioaccumulations of the test compounds. The K_{OW}-, D_{OW}- and D_{MLW}-based approaches applied the partition coefficient to predict the accumulation in the cells. RTgill-W1 and RTL-W1 BCF are calculated from the observed mass balances and the measured cell numbers and represent the *in vitro* BCFs. The rainbow trout BCF represents the *in vivo* BCF for reference.

Table S14: Predicted and measured BCFs of the test compounds. If applicable, the mean of a BCF value is presented. Since Q14 is permanently charged, no K_{OW} could be calculated and consequently no D_{OW}. The assumed lipid volume fraction in the cells for K_{OW} and D_{OW}-based calculations was 0.04 , as for whole fish (subtracting 1 % phospholipid of initially 5 % lipid volume fraction) [6, 12].

Compound	BCF type	Value (log)
T10	K_{OW}-based[1]	4.81
T10	D_{OW}-based[2]	1.21
T10	D_{MLW}-based[3]	1.64
T10	RTgill-W1	2.36
T10	RTL-W1	2.27
T10	Rainbow trout[4]	2.2
S12	K_{OW}-based[1]	5.25
S12	D_{OW}-based[2]	3.45
S12	D_{MLW}-based[3]	3.39
S12	RTgill-W1	3.57
S12	RTL-W1	3.43
S12	Rainbow trout[4]	2.96
Q14	K_{OW}-based[1]	not available
Q14	D_{OW}-based[2]	not available
Q14	D_{MLW}-based[3]	3.46
Q14	RTgill-W1	3.94
Q14	RTL-W1	4.14
Q14	Rainbow trout[4]	1.75

[1]K_{OW}-driven partitioning into cells,[2]D_{OW}-driven partitioning into cells,[3]D_{MLW}-driven partitioning into cells

Figure S6 visualizes the K_{OW} and D_{OW}-based BCF prediction in the cells compared to the observed *in vitro* BCFs. The comparison was used to assess whether K_{OW} and D_{OW} were suitable descriptors for the *in vitro* observed accumulation. Since no K_{OW} or D_{OW} was available for Q14 (fully ionized), the K_{OW} and D_{OW}-based predictions could not be performed.

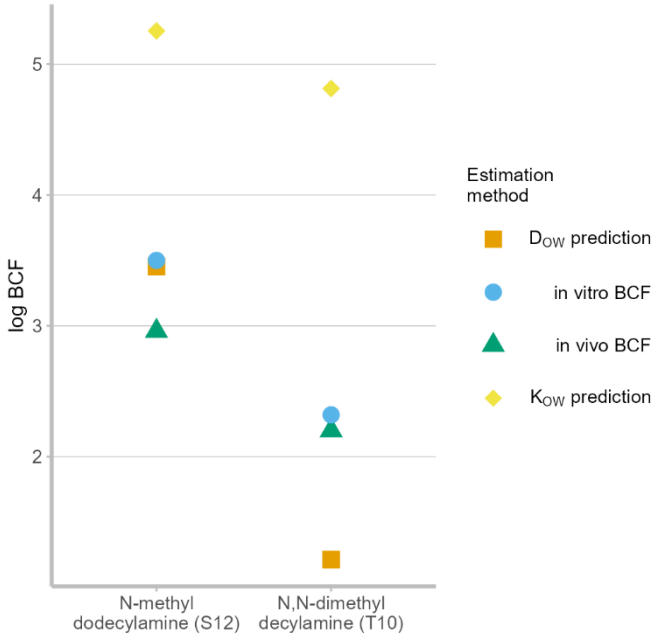

Figure S7: Comparison of *in vitro* BCF with K_{OW}- and D_{OW}-based BCF predictions in the cells. *In vitro* BCF represent the mean of experiments with RTgil-W1 and RTL-W1, while *in vivo* BCF were taken from Kierkegaard et al.[13].

8. Biotransformation analyses

8.1. Biotransformation analysis following OECD TG 319A and 319B

OECD TG319 [8, 9] criteria were applied to the mass balances to see if a clearance rate could be calculated. The results are shown in Table S15 to S17.

Table S15: Analysis for biotransformation activity of the experiments with S12 following OECD TG criteria in RTL-W1 (top) and RTgill-W1 (bottom) cell lines.

N-methyldodecylamine (S12) in RTL-W1		
	Cell-free control	Exposed Cells
R squared	0.06484	0.4517
Is slope significantly non-zero?		
F	1.109	13.18
P value	0.3078	0.0022
Deviation from zero?	Not Significant	Significant
Equation	Y = -0.0005241*X + 5.265	Y = -0.001796*X + 5.282
N-methyldodecylamine (S12) in RTgill-W1		
	Cell-free control	Exposed Cells
R squared	0.03102	0.1706
Is slope significantly non-zero?		
F	0.5122	3.29
P value	0.4845	0.0885
Deviation from zero?	Not Significant	Not Significant
Equation	Y = -0.0004272*X + 5.321	Y = -0.001429*X + 5.369

Table S16: Analysis for biotransformation activity of the experiments with T10 following OECD TG criteria in RTL-W1 (top) and RTgill-W1 (bottom) cell lines.

N,N-dimethyldecylamine (T10) in RTL-W1		
	Cell-free control	Exposed Cells
R squared	0.2717	0.3426
Is slope significantly non-zero?		
F	5.968	8.338
P value	0.0265	0.0107
Deviation from zero?	Significant	Significant
Equation	Y = -0.003935*X + 5.643	Y = -0.004492*X + 5.643
N,N-dimethyldecylamine (T10) in RTgill-W1		
	Cell-free control	Exposed Cells
R squared	0.01773	0.006749
Is slope significantly non-zero?		
F	0.2887	0.1087
P value	0.5984	0.7459
Deviation from zero?	Not Significant	Not Significant
Equation	Y = -0.0009844*X + 5.564	Y = -0.0006712*X + 5.538

Table S17: Analysis for biotransformation activity of the experiments with Q14 following OECD TG criteria in RTL-W1 (top) cell lines.

N,N,N-trimethyltetradecylammonium (Q14) in RTL-W1		
	Cell-free control	Exposed Cells
R squared	0.09055	0.003213
Is slope significantly non-zero?		
F	0.5974	0.01934
P value	0.4689	0.8939
Deviation from zero?	Not Significant	Not Significant
Equation	Y = -0.001199*X + 4.164	Y = -0.0001936*X + 5.056

8.2. Biotransformation product of T10 in RTL-W1 cells

We conducted screenings for biotransformation products and only experiments with RTL-W1 exposed to T10 indicated biotransformation activity. The screening resulted in the detection of one biotransformation product as shown in Figures S8 to S10. However, the detections were small and the amounts could not be quantified.

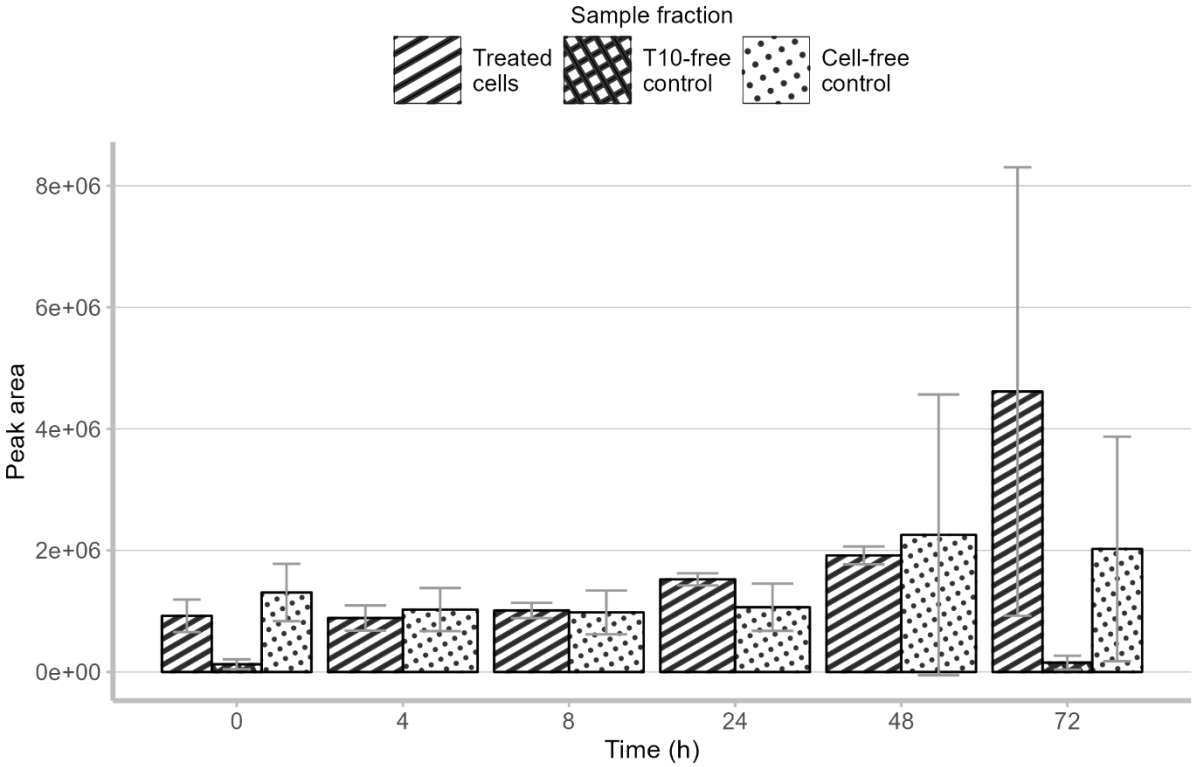

Figure S8: Detection of demethylated T10 in medium samples. Error bars mark the standard deviations.

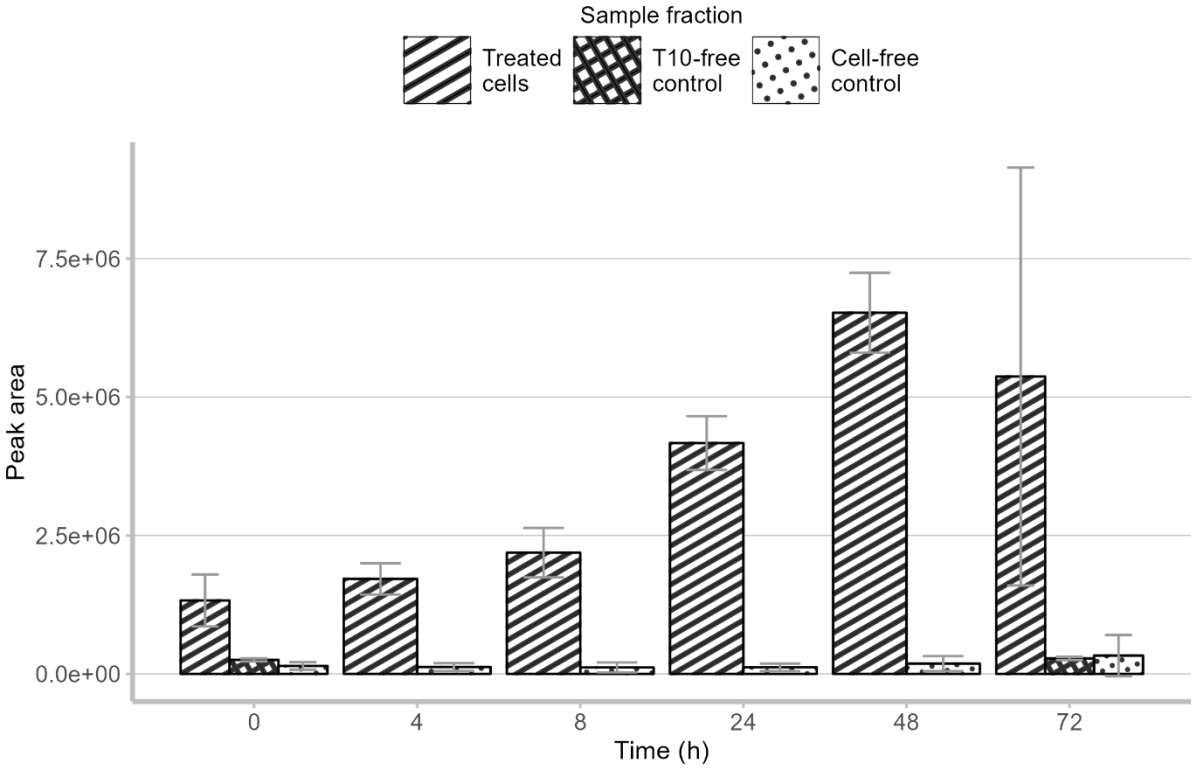

Figure S9: Detection of demethylated T10 in cell samples. Error bars mark the standard deviations.

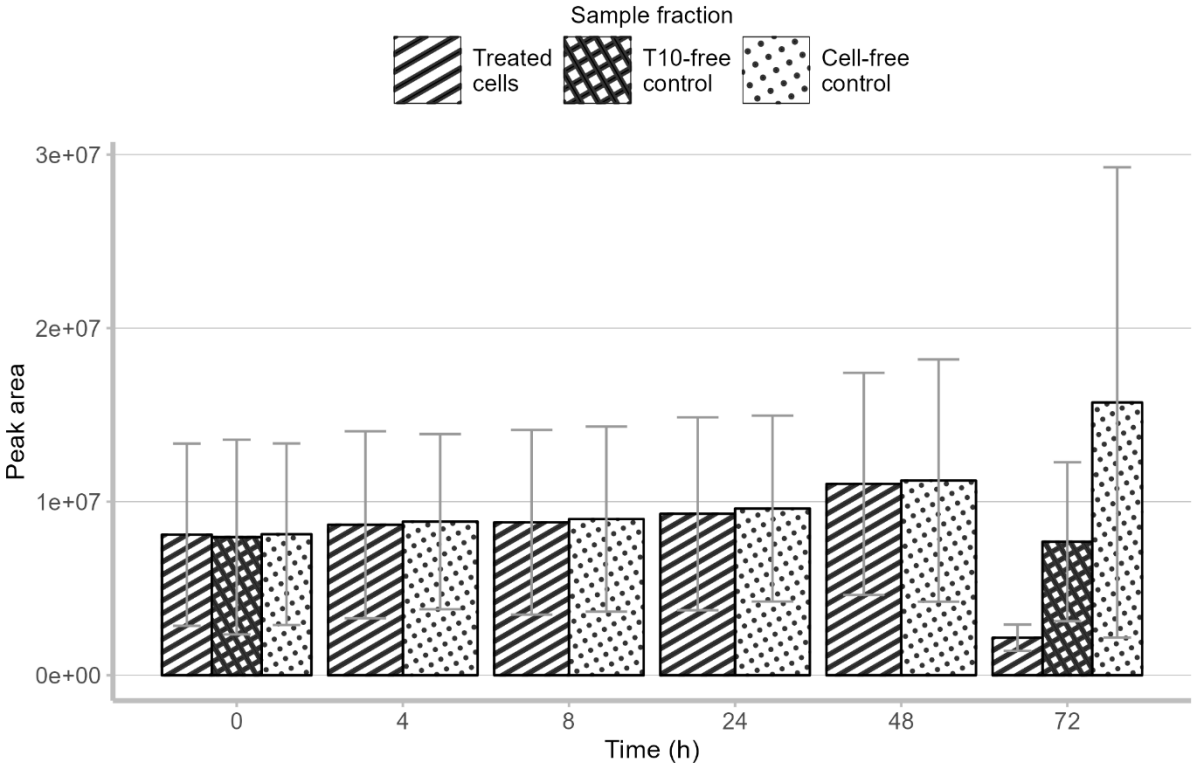

Figure S10: Detection of demethylated T10 in plastic samples. Error bars mark the standard deviations.

9. Model applications

9.1. *In vitro* mass balance model

The *in vitro* mass balance model "MBM EQP v2.0" [14] (spreadsheet available at https://arnotresearch.com/models/) was used to assess the influence of reduced bioavailability of the test compounds at steady state. The model estimates compound distribution in the different compartments of the test system, which comprises several medium constituents, plastic, cells (with several sub compartments) and the air-filled headspace.

We applied partition coefficients for lipid membrane of the neutral species and serum protein, i.e bovine serum albumin, that were derived by estimation methods (PP-LFER), which are more accurate than the default applied correction terms (see Table S18) [15,16,17]. The lipid membrane-water partition coefficients of the ionic test compounds were assumed to be close to the compound's D_{MLW} values from Timmer & Droge [18], due to negligible small influence of the neutral species at neutral pH (7). The following tables detail the relevant input data comprising the compound's physicochemical properties (Table S18), test system characteristics (Table S19) and relevant cell and medium constituents (Table S20, S21). If not specified differently in the tables, the settings for the model were kept in their default. Please note that due to the model design, we could only specify well plate formats. Therefore, we derived the metrics of our test system (cell flask with 25 cm^2 growth area) and adapted it to a well, which would have the same metrics (growth area, headspace volume etc.). The experiments were conducted in commercial Leibovitz's L15 medium, supplemented with 5 % bovine serum albumin, for which the ionic strength was calculated (Table S21). The results are presented in Table S22 and S23 and contain the relevant mass fraction and concentrations of the test system at steady state and the predicted *in vitro* based BCF. Two scenarios were used to derive predicted *in vitro* BCF. The first scenario applied the estimated free bioavailable

aqueous concentration, C_{WAT}, and the second scenario applied the estimated bulk medium concentration, $C_{BULK\ WAT}$ containing all medium constituents and water (Table S23).

Table S18: Physicochemical properties of the test compounds for model application. Except for log $K_{MW,I}$, all partition coefficients were estimated. MW = Molecular weight, MP = Melting point (EPI Suite v1.01), B = Base (IOC type), log $K_{OW,N}$ = Octanol-water partition coefficient of neutral species [15], log $K_{OW,I}$ = Octanol-water partition coefficient of ionic species (COSMOtherm or , as for Q14, correction term -3 subtracted from log $K_{OW,N}$ [19], log $K_{MW,N}$ = Membrane-water partition coefficient of neutral species [16], log $K_{MW,I}$ = Membrane-water partition coefficient of ionic species [18], log $K_{SaW,N}$ = Serum-albumin-water partition coefficient of neutral species [17], log $K_{SaW,I}$ = Serum-albumin-water partition coefficient of ionic species [17], log $K_{AW,N}$ = Air-water partition coefficient of neutral species (EPI Suite v1.01), $C_{SAT,W,N}$ = Water solubility of neutral species (EPI Suite v1.01), ECx = Exposure concentration of the bioassay

Compound	CAS RN	MW (g/mol)	MP (°C)	IOC Type	pKa	log $K_{OW,N}$	log $K_{OW,I}$	log $K_{MW,N}$	log $K_{MW,I}$	log $K_{SaW,N}$	log $K_{SaW,I}$	log $K_{AW,N}$	$C_{SAT,W,N}$ (mg L^{-1})	EC*x* (µM)
Q14	4574043	256.5	187.2	B	16.0	9.4	4.7	8.3	5.5	7.3	5.3	-9.4	0.002	0.1
T10	1120247	185.35	0.8	B	9.8	6.1	2.5	4.4	3.7	3.8	2.6	-1.7	48.4	2.2
S12	7311300	199.38	26.5	B	10.8	6.6	2.7	5.0	5.4	4.4	3.3	-1.8	13.6	0.9

Table S19: Input parameters for assay specific well plate characteristics. Please note that the volumes and areas were adapted to the measures of the plastic flasks used in our experiments.

Well diameter (bottom, mm)	Growth area (bottom, mm^2)	Total well volume (µL)	Typical working volume (µL)	Working volume (µL)	Avg. cell yield	Assumed mass of cells (mg)	Cell weight (ng/cell)
56.36	2494.96	66592.4	2500-6000	3000	3300000	0.008	2.41^{-3}

Table S20: Input parameters for system characteristics.

Proportionality constants (to octanol)	Structural protein	0.035
	Dissolved organic matter	0.05
	Storage lipid-octanol	1
Characteristics of cell/tissues	Storage lipids	0
	Membrane lipids	0.0213
	Structural protein (non-lipid organic matter)	0.09
	Density (cells)	1 kg L^{-1}
	pH	7.4
	Temperature	19 °C
Characteristics of buffer (exposure medium)	Ionic strength (see Table S21)	1.909
	pH	7
Characteristics of serum (FBS)	Albumin	16.92 g L^{-1}
	Lipids	0.84 g L^{-1}
Characteristics of serum & dissolved organic matter inputs	Volume fraction	0.05 L L^{-1}
	$C_{dissolved\ organic\ matter}$ (see Table S21)	3970.1 mg L^{-1}
	Density of dissolved organic matter	1 kg L^{-1}

Ionic strength I of the exposure medium was calculated with equation S5:

Equation S5: $$I = 0.5 \sum_{i=1}^{n} c_i x_i z_i^2$$

Where n is the total number of compounds (see Table S21), c_i the concentration of compound i (molL-1), x_i the number of atoms of compound i and z_i the charge of adduct in compound i. The calculations

based on the medium constituents detailed in Table S21 and were obtained from the manufacturer (Thermo Fisher Scientific Inc., CH).

Table S21: Medium constituents for ionic strength calculation. The dissolved organic matter above was calculated from the concentration of organic substances listed here (total 3970.1 mg L^{-1}).

Compound	g mol^{-1}	C_i (mg L^{-1})	C_i (mol L^{-1})	z_i +	Z_i -	I (mol L^{-1})
Choline chloride	140	1	7.143E-05	1	1	7.143E-05
D Calcium pantothenate	477	1	2.096E-05	2	2	6.289E-05
Folic acid	441	1	2.268E-05	0	2	2.268E-05
Pyridoxine Hydrochloride	206	1	4.854E-05	0	1	2.427E-05
Riboflavin 5'-phosphate Na	478	0.1	2.092E-06	1	1	2.092E-06
Thiamine monophosphate	442	1	2.262E-05	1	2	3.394E-05
Calcium chloride ($CaCl_2$)	111	140	0.0126126	2	2	0.0378378
Magnesium chloride	95	93.7	0.0098632	2	2	0.0394526
Magnesium sulfate ($MgSO_4$)	120	97.67	0.0081392	2	2	0.0325567
Potassium chloride (KCl)	75	400	0.0533333	1	1	0.0533333
Potassium Phosphate monobasic (KH_2PO_4)	136	60	0.0044118	1	1	0.0044118
Sodium chloride (NaCl)	58	8000	1.3793103	1	1	1.3793103
Sodium Phosphate dibasic (Na_2HPO_4)	142	190	0.0133803	2	2	0.0267606
Sodium pyruvate	110	550	0.05	1	1	0.05
Glycine	75	200	0.0266667	1	1	0.0266667
Alanine	89	225	0.0252809	1	1	0.0252809
Arginine	174	500	0.0287356	2	1	0.0431034
Asparagine	132	250	0.0189394	1	1	0.0189394
Cysteine	121	120	0.0099174	1	2	0.014876
Glutamine	146	300	0.0205479	1	1	0.0205479
Histidine	155	250	0.016129	1	1	0.016129
Isoleucin	131	250	0.019084	1	1	0.019084
Leucine	131	125	0.009542	1	1	0.009542
Lysine	146	75	0.005137	2	1	0.0077055
Methionine	149	75	0.0050336	1	1	0.0050336
Phenylalanine	165	125	0.0075758	1	1	0.0075758
Serine	105	200	0.0190476	1	1	0.0190476
Threonine	119	300	0.0252101	1	1	0.0252101
Tryptophan	204	20	0.0009804	1	1	0.0009804
Tyrosine	181	300	0.0165746	1	1	0.0165746
Valine	117	100	0.008547	1	1	0.008547

Table S22: Predicted steady state concentrations and mass fractions of the test compounds in the test system. $C_{Nom\ initial}$ = Initial nominal (measured) exposure concentration, $C_{BULK\ WAT}$ = bulk water concentration comprising all medium constituents, C_{WAT} = free aqueous water concentration in the exposure medium, C_{AIR} = concentration in air of the head space, C_{ALB} = concentration in serum albumin (in medium), $C_{S\text{-}LIP}$ = concentration in storage lipid (in medium), C_{DOM} = Concentration in dissolved organic matter (in medium), C_{cells} = concentration in cells, $MF_{BULK\ WAT}$ = Bulk water mass fraction comprising all medium constituents, MF_{WAT} = free aqueous water mass fraction in the exposure medium, MF_{AIR} = mass fraction in air of the head space, MF_{ALB} = mass fraction in serum albumin (in medium), $MF_{S\text{-}LIP}$ = mass fraction in storage lipid (in medium), MF_{DOM} = mass fraction in dissolved organic matter (in medium), MF_{cells} = mass fraction in cells, $MF_{plastic}$ = Mass fraction in plastic of the test vessel

Concentrations	**Q14**	**T10**	**S12**
$C_{NOM,initial}$ (µmol L^{-1} medium)	8.5E-02	2.2E+00	9.3E-01
$C_{BULK\ WAT}$ (µmol L^{-1} medium)	8.5E-02	2.2E+00	8.9E-01
C_{WAT} (µmol L^{-1} water)	4.3E-05	3.4E-01	7.2E-02
C_{AIR} (µmol L^{-1} air)	9.7E-29	3.1E-11	5.9E-13
C_{ALB} (µmol L^{-1} alb)	1.1E+02	1.1E+03	1.1E+03
$C_{S\text{-}LIP}$ (µmol L^{-1} lipid)	3.5E+02	5.0E+03	8.0E+02
C_{DOM} (µmol L^{-1} dissolved organic matter)	1.1E+00	2.4E+02	2.5E+01
C_{cells} (µmol L^{-1} cell)	1.6E+01	1.1E+03	1.4E+04
Mass fractions	**Q14**	**T10**	**S12**
$MF_{BULK\ WAT}$	99.9%	99.1%	95.9%
MF_{WAT}	0.1%	15.1%	7.8%
MF_{AIR}	0.0%	0.0%	0.0%
MF_{ALB}	77.5%	31.0%	73.6%
$MF_{S\text{-}LIP}$	17.3%	9.5%	3.6%
MF_{DOM}	5.1%	43.4%	10.9%
MF_{Cells}	0.051%	0.131%	3.946%
$MF_{Plastic}$	0.0%	0.7%	0.2%

Table S23: Predicted and in vitro-based BCF. The predicted BCF were derived from simulated cell and medium concentrations at steady state (see Table S22). Medium concentration were either the freely dissolved bioavailable fraction or the bulk medium concentration comprising all bound compound fractions.

Compound	**Log *in vitro* BCF (average from the two cell lines)**	**Predicted log BCF (using bioavailable fraction in medium, C_{WAT})**	**Predicted log BCF (using bulk medium concentration, $C_{BULK\ WAT}$)**
S12	3.4	5.3	4.2
T10	2.3	3.5	2.7
Q14	4.1	5.6	2.3

9.2. Kinetic cell model

In comparison to the *in vitro* mass balance model, the kinetic cell model calculates kinetic permeation of the neutral and the charged species of the test compounds [20, 21] and determines the resulting cellular accumulation with concurrent intracellular partitioning to structural proteins and membranes. Equation S6 presents the central equation of the cell model, while Table S24 details the relevant input information for all following equations. The applied partition

coefficients are the same as in section 9.1 (and using measured D_{MLW}, i.e. $K_{MLW,i}$). Similar to the above mass balance model, two scenarios for the bioavailability of the test compounds in the medium were used to derive *in vitro* BCF. The first one applied the estimated free bioavailable aqueous concentration, C_{WAT}, from the above mass balance model and the second scenario applied the estimated bulk medium concentration, $C_{BULK\ WAT}$ from above (Table S22).

Equation S6: $$BCF_{cell\ model} = \frac{k_{up}}{k_{elimination}} = \frac{\gamma_{medium.n}\ \alpha_{medium.n} + \ 10^{-3.5}\frac{N}{e^N - 1}\ \gamma_{medium.i}\ \alpha_{medium.i}}{\gamma_{cell.n}\ \alpha_{cell.n} + \ 10^{-3.5}\frac{N}{e^N - 1}\gamma_{cell.i}\ \alpha_{cell.i}} \times \frac{f_w}{F_{w.cell}}$$

Equation S7: $$N = \frac{zEF}{RT}$$

Equation S8: $$F_{w.cell} = \left(1 + D_{MLW}\ \frac{f_{PL}}{f_w} + \ D_{PW}\ \frac{f_P}{f_w}\right)^{-1}$$

Equation S9: $$\gamma_n = 10^{0.3\ I}$$

Equation S10: $$\gamma_i = 10^{0.5\ |z|\ (\frac{\sqrt{I}}{1} + \sqrt{I} - 0.3I)}$$

For comparison to the mass balance model, the total internal concentration in the cells IC (mol L^{-1}) was calculated as well:

Equation S11: $$IC = IC_w \times (f_{PL} \times D_{MLW} + f_p \times D_{PW} + f_w)$$

Table S24: Parameter description for Equations S6-11.

Symbol	Unit	Value	Description
k_{up}	m s^{-1}	-	Kinetic uptake rate
$k_{elimination}$	m s^{-1}	-	Kinetic elimination rate
$\gamma_{medium/cell.n}$	mol L^{-1}	-	Activity coefficient of the neutral species in medium or cells
$\gamma_{medium/cell.i}$	mol L^{-1}	-	Activity coefficient of the ionic species in medium or cells
$\alpha_{medium/cell.n}$	-	-	Fraction of neutral species in medium or cells (estimated by Henderson-Hasselbalch equation)
$\alpha_{medium/cell.i}$	-	-	Fraction of ionic species in the medium or cells (estimated by Henderson-Hasselbalch equation)
$10^{-3.5}\frac{N}{e^N-1}$			Permeability of the charged compound
$F_{w.cell}$	-	See Equation S8	Substance fraction in the water phase of the cell
f_{PL}	-	0.021	Volume fraction of membrane lipid in cells (taken from mammalian cell lines) [22]
f_P	-	0.093	Volume fraction of membrane lipid in cells (taken from mammalian cell lines, none known for fish cell lines) [23]
f_w	-	0.886	Volume fraction of water in cells
D_{MLW}	-	See Table S18	pH-dependent membrane lipid-water partition coefficient (pH 7.4 in cells, 7 in medium)
D_{PW}	-	See Table S18	pH-dependent structural protein-water partition coefficient (pH 7.4 in cells, 7 in medium)
E	V	-0.11	Membrane potential. Unknown for fish cell cultures. Assumed to be in range of typical values for mammalian cells (-0.02 to -0.120V) [24]
F	C mol^{-1}	96485	Faraday constant
R	J mol^{-1}	8.314	Universal gas constant
T	K	292.15	Experimental temperature
z	-	+1	Charge of the monoprotic bases
I	M	0.3	Ionic strength of the cell lumen (0.3, taken from zebrafish embryos [21]) or the medium (Table S21)
IC	M	-	Total internal concentration in cells
IC_w	M	-	Aqueous internal concentration in cells

Table S25: *In vitro* BCF compared to kinetic cell model-predicted BCF. The two model scenarios consider two scenarios for bioavailability; 1) 100% bioavailability of the exposure medium concentration, 2) only the free aqueous water concentration, C_{WAT}, in the exposure medium is bioavailable (predicted from section 9.1.

Compound	Log *In vitro* BCF (average from the two cell lines)	Predicted log BCF (only C_{WAT} bioavailable)	Predicted log BCF (100% bioavailability from medium $C_{BULK\ WAT}$)
S12	3.4	4.4	4.4
T10	2.3	2.8	2.8
Q14	4.1	1.8	6.6

10. References

(1) Stadnicka-Michalak, J.; Weiss, F. T.; Fischer, M.; Tanneberger, K.; Schirmer, K. Biotransformation of Benzo[a]pyrene by Three Rainbow Trout (Onchorhynchus mykiss) Cell Lines and Extrapolation To Derive a Fish Bioconcentration Factor. *Environmental Science & Technology* **2018b**, *52* (5), 3091-3100, DOI: 10.1021/acs.est.7b04548.

(2) Lee, L. E. J.; Clemons, J. H.; Bechtel, D. G.; Caldwell, S. J.; Han, K.-B.; Pasitschniak-Arts, M.; Mosser, D. D.; Bols, N. C. Development and characterization of a rainbow trout liver cell line expressing cytochrome P450-dependent monooxygenase activity. *Cell Biology and Toxicology* **1993**, *9* (3), 279-294, DOI: 10.1007/BF00755606.

(3) Balk, F.; Hollender, J.; Schirmer, K. Investigating the bioaccumulation potential of anionic organic compounds using a permanent rainbow trout liver cell line. *Environment International* **2023**, *174*, 107798, DOI: 10.1016/j.envint.2023.107798.

(4) ChemicalBook. *Ethylenediaminetetraacetic acid (EDTA)– Physical Properties and Applications*. https://www.chemicalbook.com/Article/Ethylenediaminetetraacetic-acid-EDTA-Physical-Properties-and-Applications.htm#:~:text=Physical%20Properties%20of%20EDTA&text=EDTA%20is%20white%20powder%2C%20which,ethanol%20and%20general%20organic%20solvents., (accessed 13.12.2022).

(5) DFG. Ethylendiamintetraessigsäure (EDTA) und ihre Alkalisalze [MAK Value Documentation in German language, 2009]. In *The MAK-Collection for Occupational Health and Safety: Annual Thresholds and Classifications for the Workplace*; Greim, H., Ed.; Wiley-VCH Verlag GmbH & Co, 2012; pp 1-33. DOI: 10.1002/3527600418.mb6000d0046.

(6) Hendriks, A. J.; van der Linde, A.; Cornelissen, G.; Sijm, D. T. H. M. The power of size. 1. Rate constants and equilibrium ratios for accumulation of organic substances related to octanol-water partition ratio and species weight. *Environmental Toxicology and Chemistry* **2001**, *20* (7), 1399-1420, DOI: 10.1002/etc.5620200703.

(7) Johnson, S. M.; Buttress, N. The osmotic insensitivity of sonicated liposomes and the density of phospholipid-cholesterol mixtures. *Biochimica et Biophysica Acta (BBA) - Biomembranes* **1973**, *307* (1), 20-26, DOI: 10.1016/0005-2736(73)90021-7.

(8) OECD. Test No. 319A: Determination of in vitro intrinsic clearance using cryopreserved rainbow trout hepatocytes (RT-HEP). In *OECD Guidelines for the Testing of Chemicals, Section 3* OECD Publishing, 2018a.

(9) OECD. Test No. 319B: Determination of in vitro intrinsic clearance using rainbow trout liver S9 sub-cellular fraction (RT-S9). In *OECD Guidelines for the Testing of Chemicals, Section 3* OECD Publishing, 2018b.

(10) Chen, Y.; Hermens, J. L. M.; Jonker, M. T. O.; Arnot, J. A.; Armitage, J. M.; Brown, T.; Nichols, J. W.; Fay, K. A.; Droge, S. T. J. Which Molecular Features Affect the Intrinsic Hepatic Clearance Rate of Ionizable Organic Chemicals in Fish? *Environmental Science & Technology* **2016**, *50* (23), 12722-12731, DOI: 10.1021/acs.est.6b03504.

(11) Droge, S. T. J.; Armitage, J. M.; Arnot, J. A.; Fitzsimmons, P. N.; Nichols, J. W. Biotransformation Potential of Cationic Surfactants in Fish Assessed with Rainbow Trout Liver S9 Fractions. *Environmental Toxicology and Chemistry* **2021**, *40* (11), 3123-3136, DOI: 10.1002/etc.5189.

(12) Stadnicka-Michalak, J.; Tanneberger, K.; Schirmer, K.; Ashauer, R. Measured and Modeled Toxicokinetics in Cultured Fish Cells and Application to In Vitro - In Vivo Toxicity Extrapolation. *PLOS ONE* **2014**, *9* (3), e92303, DOI: 10.1371/journal.pone.0092303.

(13) Kierkegaard, A.; Sundbom, M.; Yuan, B.; Armitage, J. M.; Arnot, J. A.; Droge, S. T. J.; McLachlan, M. S. Bioconcentration of Several Series of Cationic Surfactants in Rainbow Trout. *Environmental Science & Technology* **2021**, *55* (13), 8888-8897, DOI: 10.1021/acs.est.1c02063.

(14) Armitage, J. M.; Sangion, A.; Parmar, R.; Looky, A. B.; Arnot, J. A. Update and Evaluation of a High-Throughput In Vitro Mass Balance Distribution Model: IV-MBM EQP v2.0. *Toxics* **2021**, *9* (11), DOI: 10.3390/toxics9110315.

(15) Endo, S.; Brown, T. N.; Goss, K.-U. General Model for Estimating Partition Coefficients to Organisms and Their Tissues Using the Biological Compositions and Polyparameter Linear Free Energy Relationships. *Environmental Science & Technology* **2013**, *47* (12), 6630-6639, DOI: 10.1021/es401772m.
(16) Bittermann, K.; Spycher, S.; Goss, K.-U. Comparison of different models predicting the phospholipid-membrane water partition coefficients of charged compounds. *Chemosphere* **2016**, *144*, 382-391, DOI: 10.1016/j.chemosphere.2015.08.065.
(17) Henneberger, L.; Goss, K.-U.; Endo, S. Equilibrium Sorption of Structurally Diverse Organic Ions to Bovine Serum Albumin. *Environmental Science & Technology* **2016a**, *50* (10), 5119-5126, DOI: 10.1021/acs.est.5b06176.
(18) Timmer, N.; Droge, S. T. J. Sorption of Cationic Surfactants to Artificial Cell Membranes: Comparing Phospholipid Bilayers with Monolayer Coatings and Molecular Simulations. *Environmental Science & Technology* **2017**, *51* (5), 2890-2898, DOI: 10.1021/acs.est.6b05662.
(19) Armitage, J. M.; Arnot, J. A.; Wania, F.; Mackay, D. Development and evaluation of a mechanistic bioconcentration model for ionogenic organic chemicals in fish. *Environmental Toxicology and Chemistry* **2013**, *32* (1), 115-128, DOI: 10.1002/etc.2020.
(20) Fu, W.; Franco, A.; Trapp, S. Methods for estimating the bioconcentration factor of ionizable organic chemicals. *Environmental Toxicology and Chemistry* **2009**, *28* (7), 1372-1379, DOI: 10.1897/08-233.1.
(21) Bittner, L.; Klüver, N.; Henneberger, L.; Mühlenbrink, M.; Zarfl, C.; Escher, B. I. Combined Ion-Trapping and Mass Balance Models To Describe the pH-Dependent Uptake and Toxicity of Acidic and Basic Pharmaceuticals in Zebrafish Embryos (Danio rerio). *Environmental Science & Technology* **2019**, *53* (13), 7877-7886, DOI: 10.1021/acs.est.9b02563.
(22) Fischer, F. C.; Henneberger, L.; König, M.; Bittermann, K.; Linden, L.; Goss, K.-U.; Escher, B. I. Modeling Exposure in the Tox21 in Vitro Bioassays. *Chemical Research in Toxicology* **2017**, *30* (5), 1197-1208, DOI: 10.1021/acs.chemrestox.7b00023.
(23) Fischer, F. C.; Henneberger, L.; Schlichting, R.; Escher, B. I. How To Improve the Dosing of Chemicals in High-Throughput in Vitro Mammalian Cell Assays. *Chemical Research in Toxicology* **2019**, *32* (8), 1462-1468, DOI: 10.1021/acs.chemrestox.9b00167.
(24) Alberts, B.; Johnson, A.; Lewis, J.; Raff, M.; Roberts, K.; Walter, P. Part IV Internal Organization of the Cell: Membrane Structure. In *Molecular Biology of the Cell* 5ed.; WILEY-VCH Verlag GmbH & Co KgaA, 2011.